Heating of two-dimensional electrons by a high electric field in a quantizing magnetic field: Consequences in Landau emission and in the quantum Hall effect

C. Chaubet, A. Raymond, and D. Dur
Groupe d'Etude des Semiconducteurs URA CNRS 357, Université Montpellier II, place Eugene Bataillon, 34095 Montpellier Cedex 05, France
(Received 20 April 1995)

We study the electric-field-induced heating process of a two-dimensional electron gas in the quantum-Hall-effect (QHE) regime. We present both theoretical and experimental results. We calculate the inter-Landau-level transition probabilities under high electric field, in the presence of both phonon and impurity scattering. We deduce from the theoretical investigations the total emitted power of the cyclotron emission as a function of the electric-field intensity. We perform both cyclotron emission and quantum transport experiments, on $Ga_xAl_{1-x}As/GaAs$ and $Ga_xIn_{1-x}As/GaAs$ heterojunctions, at liquid-helium temperature and magnetic fields up to 8 T, using samples with different geometry. We therefore distinguish several cyclotron emission regimes and we demonstrate, with theoretical arguments, that the average electric field in the sample is not a good physical parameter in the description of the heating process and of the cyclotron emission for a two-dimensional electron gas. We finally present experimental results which tend to prove that the local electric field can be high enough in some parts of the sample, to induce inter-Landau-level scattering, and consequently to generate the cyclotron emission and to induce the breakdown of the quantum Hall effect. The role of the microscopic local electric field is confirmed by the observation of the emitted power amplification in the plateaus regime of the QHE. This phenomenon is due to the modification of the current path geometry and the enhancement of the local electric field in the vicinity of the contact point in the QHE regime.

I. INTRODUCTION

Landau emission (or cyclotron emission) is a very powerful tool for investigating semiconductor properties in the far-infrared (FIR) frequency range.[1–8] The electrons of a two-dimensional (2D) or 3D carrier plasma are heated up, under quantizing magnetic field, to the upper Landau levels. One can then observe the radiative recombinations of those excited electrons. The problem of the heating of 3D electrons by an electric field in Landau emission has been studied some years ago by Gornik[1–4] and Kobayashi.[5] For the Landau emission in 2D structures,[6–8] the heating process of the confined electrons by an in-plane electric field has not been studied up to now as far as we know. The problem lies in the fact that the electric field applied in the plane of an ideal two-dimensional electron gas (2DEG) at 0 K cannot accelerate electrons, because of the total quantization of the 2D gas. It is then surprising that the electric voltages applied to generate the emission in 2D and 3D samples (of comparable dimensions), should be of the same order of magnitude.[1–7] Let us also recall that the distribution of the electrostatic potential in 2D structures is highly inhomogeneous in quantum-Hall-effect (QHE) regime,[9–16,52] which complicates matters. The present work tends to give a response to the question of heating of 2D electrons by an electric field, in the Landau emission regime.

Electron heating of a two-dimensional electron gas by high electric field in the quantum-Hall-effect regime has been the subject of intense experimental and theoretical studies in the past few years.[16–25] It is well known that in the regime of the Hall plateaus, the increase of the applied electric field has two spectacular consequences: the breakdown of the QHE,[16–25,52] and the generation of the Landau emission.[6–8] At this point, at least two available models have been proposed to explain the breakdown of the QHE: (i) the quantum inter-Landau-levels scattering (QUILLS) process,[19–23] which can explain the electronic occupation of the entire Landau-levels scale, and as a consequence, the loss of the total quantization. (ii) The second model has been proposed by Dyakonov *et al.*,[16,25] who demonstrate that the nonlinearity of the current-voltage characteristic in the plateau regime is inherent to the electrostatic characteristics of the 2D electron-gas system.

The QUILLS is obviously the basic mechanism of the Landau emission in a two-dimensional structure: when the electric-field intensity is high enough, it induces efficient scattering processes between Landau levels, and causes the loss of the total quantization.[19–23] Then, radiative recombinations between Landau levels occur.

In this paper, we develop calculations of the QUILLS efficiency in the 2DEG of GaAs modulation-doped heterojunctions, and we deduce the spontaneous emitted radiation power as a function of the electric field. The paper is organized in the following way: in a large theoretical Sec. II, we calculate the inter Landau-levels transition probabilities as a function of the electric-field intensity; we deduce numerically the cyclotron emission power of the 2DEG in the case of a GaAs modulation doped heterojunction. We present our experimental results in Sec. III, and we discuss the physical processes involved in the Landau emission of 2DEG as well as the importance of the microscopic electric field, the role of

the potential inhomogeneities, and the role of contacts. We conclude in Sec. IV.

II. THEORETICAL BACKGROUND

A. Landau levels in crossed electric and magnetic fields

Let us consider a 2D gas—of dimensions L_x and L_y—of noninteracting electrons confined near the interface of a $Ga_xAl_{1-x}As$-GaAs heterojunction by an electrostatic potential $U(z)$. Let us then apply crossed electric and magnetic fields ($F\|x, B\|z$). In the absence of scattering (i.e., in the regime of plateaus of the QHE) F represents the Hall field that is perpendicular to the drift current flowing along the y direction.

When the electric-field interaction terms are not treated as perturbations, the Hamiltonian of the system is

$$H=\frac{(\mathbf{p}+e\,\mathbf{A})^2}{2m^*}+e\mathbf{F}\cdot\mathbf{r}+U(z)\ , \tag{1}$$

where $U(z)$ is the confining potential at the interface of the heterojunction (later on we will consider it as a triangular potential). Using the Landau gauge, the eigenfunctions and the eigenenergies are given by[26]

$$\nu(\mathbf{r})=\langle n,k_y|\mathbf{r}\rangle=\chi_i(z)\frac{e^{ik_y y}}{\sqrt{L_y}}\Phi_n(x-X_\nu)\ , \tag{2}$$

$$\varepsilon_{n,k_y}=(n+1/2)\hbar\omega_c+eFX_\nu+\frac{1}{2}m^*V^2\ , \tag{3}$$

where χ_i is the ith electric subband eigenfunction, Φ_n the nth harmonic-oscillator function centered on

$$X_\nu=-\left[\frac{\hbar k_y}{m^*\omega_c}+\frac{eF}{m^*\omega_c}\right]\ . \tag{4}$$

We used the classical definitions for the cyclotron pulsation $\omega_c=eB/m^*$, and for the drift velocity $V=F/B$. The values of k_y are quantized according to periodic limit conditions:

$$k_y=\frac{2\pi p}{L_y}\ ,$$

with a p integer.

An elementary investigation shows that the distribution of allowed ν states on the k_y axis is a quasicontinuum; the density of states is

$$g(\varepsilon)=\frac{L_y}{\pi\hbar V}\ . \tag{5}$$

These eigenfunctions are composed of an envelope part along the z axis, which derives from the triangular potential at the interface, and an in-plane function, so that both movements can be treated independently. These movements are anyway coupled in case of scattering processes. The plane-wave part $e^{ik_y y}$ of the wave functions accounts for the drift current which flows with the velocity V along the Y axis, in the direction perpendicular to both electric and magnetic fields. In the absence of scattering, the current density corresponds to this drift current and is perpendicular to the electric field, which corresponds, in this configuration, to the Hall field: this is the Hall plateau regime and the electrons motion does not involve any dissipation. On the contrary, in the presence of scattering that involves wave-vector exchange, the orbit center is perpetually shifted [Eq. (4)] in the field direction; the current density is the sum of the drift current and of a "hopping" current in the electric-field direction. Then the current density is not perpendicular to the electric field and the dissipation occurs.

Equation (3) shows that, in the presence of an electric field in the X direction, the Landau energies of the unperturbed Landau levels (LL's) are enlarged by a field-dependent term, which is a function of the k_y wave vector, and are now dependent of two quantum numbers n and k_y. This means that the electrostatic potential suppresses the degeneracy of the LL. We have depicted this quantum system in Fig. 1: the energies of electronic states vary linearly with the cyclotron orbit center (X_ν) or with the plane wave vector k_y [see Eq. (4)]. The Fermi level, which is not a constant out of the thermal equilibrium, varies like the electrostatic potential,[27] and, as a consequence, all the $|n,k_y\rangle$ states of equal n are equally occupied.[26,28] One can see in Fig. 2, that in the presence of an electric field, the overlap of the eigenfunctions of different Landau levels n is not necessarily zero, and electrons can be scattered from one Landau level to another, due to processes that can be elastic or not. The stronger the electric field, the more important the overlap between two given states, and the more efficient the scattering. In the general case, the scattering involves an exchange of both energy and wave vector, and, as mentioned above, shifts the orbit center along the X axis. The appearance of a current component in the electric-field direction induces the onset of dissipation in the quantum-Hall-effect regime.[19–23] Concerning the Landau emission problem,

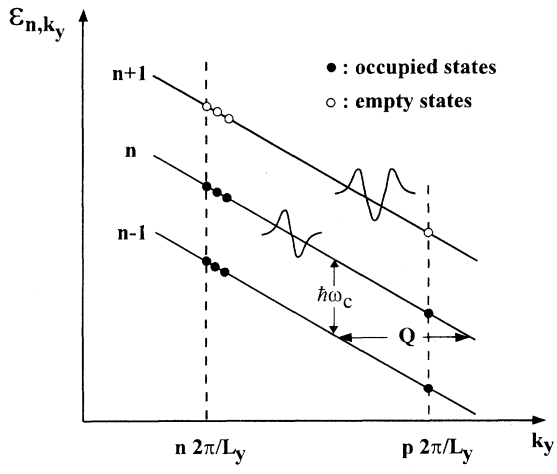

FIG. 1. Quantum eigenstates of a two-dimensional electron gas in crossed electric and magnetic fields ($F\|X; B\|Z$). k_y represents the wave vector of the plane-wave part $e^{ik_y y}$ of the eigenfunction.

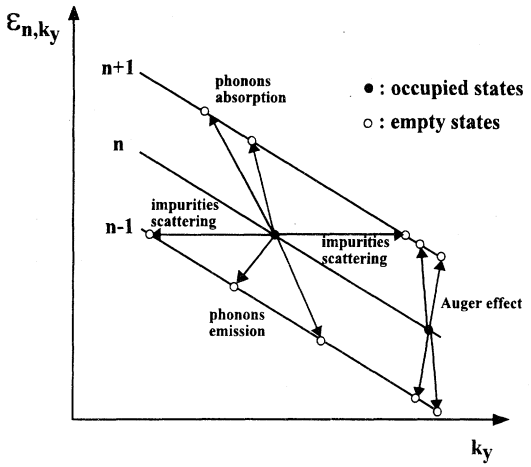

FIG. 2. Possible quantum inter-Landau-levels scattering processes.

when the electric field is high enough for QUILLS processes to be more efficient than the radiative recombination processes (which maintain the electrons in the lowest levels), the 2D electrons can populate the Landau ladder. A totally different electronic distribution is, therefore, obtained under electric field; this is what we calculate in the next paragraph. We will, therefore, deduce from this distribution the characteristics of the radiative emitted power.

B. QUILLS probabilities

We calculate, in this part, the transition probabilities of different scattering processes and we discuss their physical role, in the generation of the cyclotron emission. For a given scattering process, which generally involves both energy and momentum and thus couples two states $\nu=|n,k_y\rangle$ and $\mu=|n',k_y'\rangle$, one can calculate the transition probability using the Fermi golden rule, in the Born approximation:

$$W_{\nu\to\mu}=\frac{2\pi}{\hbar}|\langle\nu|H_{\rm int}|\mu\rangle|^2\delta(\varepsilon_\mu-\varepsilon_\nu)\ , \tag{6}$$

where $H_{\rm int}$ is the scattering Hamiltonian.

In the following we study separately, the acoustic-phonon scattering, the optical-phonon scattering, the impurity scattering, the Auger effect (due to electron-electron scattering), and the radiative recombination process.

1. *Acoustic electron-phonon interaction*

The acoustic-phonon interaction was first evocated as being the origin of the dissipation effect in the plateau regime of the QHE:[19–23] one can refer to the paper of Heinonen, Taylor, and Girvin[20] who calculated the current density that induces the breakdown of the QHE, in a model which takes into account both piezoelectric and deformation-potential interactions . Since GaAs is a piezoelectric semiconductor,[29] we should take into account this interaction, as well as the deformation-potential one.[30] But previous studies on $Ga_xAl_{1-x}As$-GaAs heterojunctions (Ref. 31 and references therein) have concluded that the deformation-potential interaction is dominant in the carrier density range $(1-6)\times10^{11}$ cm^{-2}. We will just use the argument that those two interactions are of the same order of magnitude for a 2DEG in GaAs, and develop a complete description of the deformation-potential interaction, neglecting the piezoelectric interaction, in order to provide a first approach of the understanding of the 2DEG cyclotron emission.

The choice of the initial and final states $\nu=|n,k_y\rangle$ and $\mu=|n',k_y'\rangle$ fixes both momentum and energy exchange, so that the characteristics of the phonon involved in the process are given by $q_y=k_y'-k_y$, $\varepsilon_{\rm ph}(q)=\varepsilon_\mu-\varepsilon_\nu$ (see Fig. 3). The condition $|\mathbf{q}|=\sqrt{q_x^2+q_y^2+q_z^2}=\varepsilon_\mu-\varepsilon_\nu/\hbar c_s>q_y$ (i.e., $\varepsilon_\mu-\varepsilon_\nu>\hbar c_s q_y$) must be verified in order to ensure the existence of the absorbed or emitted phonon. Let us remark that the two components q_x and q_z couple the movements in the three space directions. Finally, we consider as valid the Debye model: $\varepsilon(q)=\hbar c_s q$.

In this case, energy and momentum are correlated by the following group of relations:

$$q=\pm\frac{\omega}{c_s}\pm\frac{V}{c_s}q_y\ , \tag{7}$$

where the sign depends on the considered processes that are represented in Fig. 3 (processes 1–4).

For the deformation-potential interaction, one can write[32]

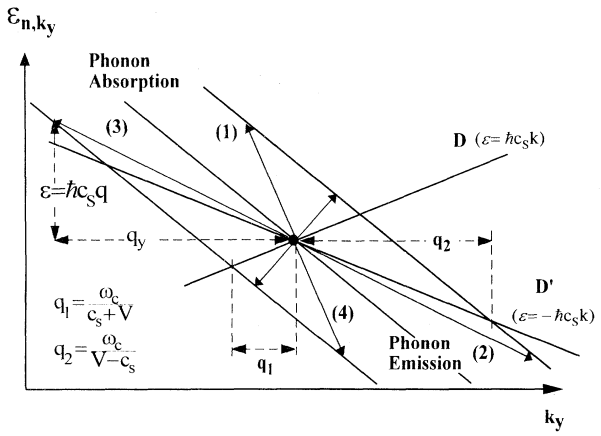

FIG. 3. Phonon-scattering processes between Landau levels. From a given initial state, the possible final states on adjacent levels are located above the lines D and D', or below these lines. In the first case there is phonon absorption, in the latter, phonon emission. q_1 and q_2 are extremal values of the exchange Y component of the phonon wave vector.

$$W_{\nu\to\mu}(q_y)=\frac{2\pi}{\hbar}\sum_{\text{q,at given } q_y} C(q)^2|f_{\nu\mu}(\mathbf{q})|^2 \times\delta(\varepsilon_\mu-\varepsilon_\nu\pm\hbar c_s q)\ , \quad (8)$$

where $|f_{\nu\mu}(\mathbf{q})|^2=|\langle\nu|e^{i\mathbf{q}\cdot\mathbf{r}}|\mu\rangle|^2$ is the form factor of the electronic states ν and μ (we report in the Appendix the calculations of those terms).

For the phonon absorption process, $C(q)$ is

$$C(q)=\left[\frac{\hbar n_q}{2\mu_\nu\Omega\omega_q}\right]^{1/2} qE_1\ . \quad (9)$$

Then for the emission process

$$C(q)=\left[\frac{\hbar(n_q+1)}{2\mu_\nu\Omega\omega_q}\right]^{1/2} qE_1\ .$$

E_1 is the deformation potential,[32] Ω the electron-gas volume, μ_ν the mass density, ω_q the phonon pulsation, n_q the occupation number of phonons in the q state. In our calculations, we took $E_1=12$ eV.[31,33]

The sum over all the q vectors of a given q_y can be expressed as an integral over q_x and q_z:

$$W_{\nu\to\mu}(q_y)=\frac{2\pi}{\hbar}\int_{q_x,q_z}\frac{\hbar n_q E_1^2}{2\mu_\nu\Omega c_s}q|f_{\nu\mu}(\mathbf{q})|^2\frac{L_xL_z dq_x dq_z}{(2\pi)^2} \times\delta(\varepsilon_\mu-\varepsilon_\nu-\hbar c_s q)\ , \quad (10)$$

where L_z is a characteristic dimension of the well in the z direction.

If we change the system of variables,

$$q_\perp=\sqrt{q^2-q_y^2}\ ,$$

$$q_z=q_\perp\cos\theta\ ,$$

$$q_x=q_\perp\sin\theta\ ,$$

the equation takes the following form:

$$W_{\nu\to\mu}(q_y)=\frac{L_xL_zE_1^2}{4\pi\mu_\nu\Omega c_s^2\hbar}\int_{q_\perp,\theta}n_q q|f_{\nu\mu}(q_\perp,\theta)|^2 \times\delta(q-q_0)q_\perp dq_\perp d\theta\ , \quad (11)$$

with

$$q_0=\frac{\varepsilon_\mu-\varepsilon_\nu}{\hbar c_s}\ .$$

Performing the integration over the q variable, we can write this probability as

$$W_{\nu\to\mu}(q_y)=\frac{L_xL_zE_1^2}{4\pi\mu_\nu\Omega c_s^2\hbar}n_q q_0^2\int_{\theta=0}^{2\pi}|f_{\nu\mu}(q_0,\theta)|^2 d\theta\ . \quad (12)$$

The transition probabilities between the "n" and "$n+1$" Landau levels are then obtained by summing over q_y. One can write

$$W_{n,n+1}=\int_{q_y}W_{\nu\to\mu}(q_y)\frac{dq_y}{2\pi/L_y}\ .$$

This leads to the following final equation:

$$W_{n,n+1}=\frac{E_1^2}{8\pi^2\mu_\nu c_s\hbar v}\times\left\{\int_{q_1}^{\infty}n_q q^2\left[\int_{\theta=0}^{2\pi}|f_{\nu\mu}(q,\theta)|^2 d\theta\right]dq + \int_{q_2}^{\infty}(n_q+1)q^2\times\left[\int_{\theta=0}^{2\pi}|f_{\nu\mu}(q,\theta)|^2 d\theta\right]dq\right\}\ , \quad (13)$$

which can be calculated using numerical methods. The probability $W_{n+1,n}$ can be obtained by interchanging q_1 and q_2 in the above formula (see Fig. 3).

2. *Optical electron-phonon interaction*

Although optical phonons do not statistically exist at liquid-helium temperature, they can be emitted by numbers in the following case: under high enough electric field, the electrons which populate the entire Landau ladder immediately recombine emitting an optical phonon if the difference between their energy and the one of an unfilled LL is larger than the longitudinal optical-phonon energy $\hbar\omega_{\mathrm{LO}}$.[28,17] As a consequence of the high efficiency of this scattering process, the lifetime of electrons on upper LL [those for which $(n+1/2)\hbar\omega_c>\hbar\omega_{\mathrm{LO}}$] vanishes. For us this interaction limits de facto the total number of the Landau levels that can be populated. We could verify *a posteriori* this physical assumption, as discussed in Sec. III B. We took in our calculations $\hbar\omega_{\mathrm{LO}}=36.2$ meV.[34]

3. *Electron-ionized impurities interaction*

The elastic diffusion on the charged impurities has been suggested as a possible mechanism for the QUILLS by Heinonen, Taylor, and Girvin,[20] but it has not been treated up to now. We develop now the calculations of the inter-Landau-levels transition probabilities assisted by ionized impurity scattering. We considered both residual impurities in the well, and the ones that have been intentionally introduced behind the spacer in the $Ga_xAl_{1-x}As$ layer and that are ionized at the thermal equilibrium.

In the general case, the scattering process assisted by ionized impurities is elastic and involves only momentum exchange (Fig. 2). The states that can be involved in this scattering process have necessarily the same energy; the momentum exchange is then (see Fig. 1)

$$Q=\Delta k_y=\frac{\omega_c}{V}\ . \quad (14)$$

Let us first consider the case of the barrier impurities. We suppose that the ionized centers are located at R_i and scatter independently the electrons. The Coulomb potential seen by an electron is then $V(r)=\sum_i v(r-R_i)$, where $v(r)$ is the Coulomb potential decreasing like $1/r$.

The inter-Landau-level transition probability, due to scattering by ionized barrier impurities is

$$W_{\nu\to\mu}=\frac{2\pi}{\hbar}\left|\int_r d^3r|\chi_0(z)|^2\varphi_\nu(\mathbf{r}_\perp)\varphi_\mu(\mathbf{r}_\perp)V(\mathbf{r})\right|^2 g(\varepsilon)\ , \tag{15}$$

where φ_ν,φ_μ are the electronic eigenfunctions in the xy plane, and $g(\varepsilon)$ the density of states [Eq. (5)]. $\chi_0(z)$ is the envelope function of the first electric subband.

The electrical potential of one impurity can be written using the plane Fourier transform,

$$V(\mathbf{r})=\int_{\mathbf{q}_\perp}\frac{Sd^2q_\perp}{(2\pi)^2}V_i(z,q_\perp)e^{i\mathbf{q}_\perp\cdot\mathbf{r}_\perp}\ , \tag{16}$$

where S is the surface of the system. Then, the transition rate can be expressed as

$$W_{\nu\to\mu}=\frac{2\pi}{\hbar}\left|\int_{\mathbf{q}_\perp}d^2q_\perp\frac{S}{(2\pi)^2}\int_{\mathbf{r}_\perp}d^2r_\perp\varphi_\nu(\mathbf{r}_\perp)\varphi_\mu(\mathbf{r}_\perp)e^{i\mathbf{q}_\perp\cdot\mathbf{r}_\perp}F_i(\mathbf{q}_\perp,z_i)\right|^2\delta(\varepsilon_\nu-\varepsilon_\mu)\ , \tag{17}$$

where

$$F_i(\mathbf{q}_\perp,z_i)=\int_z dz\chi_0^2(z)V_i(z,\mathbf{q}_\perp) \tag{18}$$

is a form factor already calculated by Ando, Fowler, and Stern:[35]

$$F_i(\mathbf{q}_\perp,z)=\frac{e^2}{2S\varepsilon_r\varepsilon_0(q_\perp+q_s)}\int_{-\infty}^{+\infty}\chi_0^2(z)e^{-q_\perp|z-z_i|}dz\ . \tag{19}$$

z_i is the position of the ith impurity on the z axis, q_s is the screening parameter that can be calculated by[36]

$$q_s=\frac{2m^*e^2}{4\pi\varepsilon_0\varepsilon_r\hbar^2}\approx 2.3\times10^8\ \mathrm{m}^{-1}\ \text{(in GaAs)}\ . \tag{20}$$

The above integral can be analytically calculated by using a simplifying hypothesis: we assume that the ionized impurities are located at a distance from the interface equal to the spacer thickness (z_0), and that their density is equal to the 2D electronic population in the well enlarged by the depletion density (N_s+N_{dep}), to account for the charge conservation in the structure.

In Eq. (17), we can change the $q_\perp$ integral in a q_x one, assuming that $q_y=\omega_c/V$. One obtains

$$W_{\text{barrier impurity}}=\frac{2(N_s+N_{\mathrm{dep}})L_x}{V}\left[\frac{e^2}{8\pi^2\varepsilon_r\varepsilon_0\hbar}\right]\times\left|\int_{q_x}\frac{e^{-qz_0}}{(q_\perp+q_s)\left[1+\frac{q_\perp}{b}\right]^3}f_{\nu\mu}(q_\perp)dq_x\right|^2\ . \tag{21}$$

$f_{\nu\mu}(q_\perp)$ is given in the Appendix by the third term that does not depend on q_z. This integral is now numerically calculable.

We consider now the case of the residual impurities in the well. The inter-Landau-level probabilities for transition assisted by ionized impurities in the well is written[32]

$$W=\frac{2\pi}{\hbar}\frac{N_i}{\Omega}\sum_q|w(q)|^2|\langle\nu|e^{i\mathbf{q}\cdot\mathbf{r}}|\mu\rangle|^2\delta(\varepsilon_\mu-\varepsilon_\nu)\ , \tag{22}$$

where N_i is the volumic density of charge; $W(q)$ is the 3D Fourier transform of $V(r)$,

$$W(q)=\frac{e^2}{\varepsilon_r\varepsilon_0q^2}\ .$$

Introducing the density of states, one obtains

$$W_{\text{well imp.}}=2\left[\frac{e^2}{\varepsilon_r\varepsilon_0\hbar}\right]^2\frac{N_I}{(2\pi)^3V}\times\int_{q_x,q_y}\frac{1}{q^4}|f_{\nu\mu}(\mathbf{q})|^2dq_xdq_y\ . \tag{23}$$

4. *Auger effect*

In the Auger effect process, the energy released by an electron relaxing to a lower-lying state is transferred to another electron, excited onto a higher state.[2] This effect has been observed within Landau levels in a two-dimensional electron gas. In this recombination process, the energy and momentum of the two-electrons system are conserved: neither energy nor momentum is transferred to the lattice.

Helm *et al.*[37] and Muro *et al.*[38] have measured the Landau-level electron lifetime in similar heterostructures: they found a strong dependence in the electron concentration and attributed this effect to this electron-electron interaction. But, it is obvious that this process is only possible if the electrons are not all confined in the bottom of the Landau ladder. Free states must exist in the lower levels in order to permit one of the two electrons to release its energy. Therefore, this scattering is very important only when the electrons begin to be equally distributed on the Landau ladder. So we consider the Auger effect as an additional pumping process when other scattering processes have already changed the equilibrium. We shall then consider its contribution only as a final process of electron repartition onto the Landau ladder.

5. *Radiative recombination*

Spontaneous photon emissions occur as soon as free states exist in the lower levels. The transition probability is given by the Fermi golden rule:

$$W_{n+1\to n}=\frac{2\pi}{\hbar}\int_k |\langle\varphi_{n+1}|H_{\rm int}|\varphi_n\rangle|^2 \times\delta(\varepsilon_{n+1}-\varepsilon_n-\hbar\omega_c)\frac{\Omega d^3k}{(2\pi)^3}\ , \tag{24}$$

and $H_{\rm int}$ is the electron photon interaction Hamiltonian:

$$H_{\rm int}=e\frac{\mathbf{A}_{\rm rad}\cdot\mathbf{P}}{m^*}\ , \tag{25}$$

where $\mathbf{A}_{\rm rad}$ is the potential vector of the emitted radiation, and $\mathbf{P}$ is the electron momentum in the static magnetic field.

The matrix element over two neighbor Landau levels is then[39]

$$\langle\varphi_{n+1}|H_{\rm int}|\varphi_n\rangle=\frac{eA_0\hbar}{m^*L}\sqrt{n+1}\ , \tag{26}$$

where the magnetic length is $L=\sqrt{\hbar/eB}$. The electron amplitude radiation is given by the quantum electrodynamics:[40]

$$A_0=\left[\frac{\hbar}{2\varepsilon_0\omega\Omega}\right]^{1/2}\ , \tag{27}$$

where Ω is the volume and ω the radiation pulsation. Integrating over q, one obtains

$$W_{n+1\to n}=\frac{e^4B^2\sqrt{\varepsilon_r}}{2\pi\varepsilon_0c^3m^{*3}}(n+1)\ , \tag{28}$$

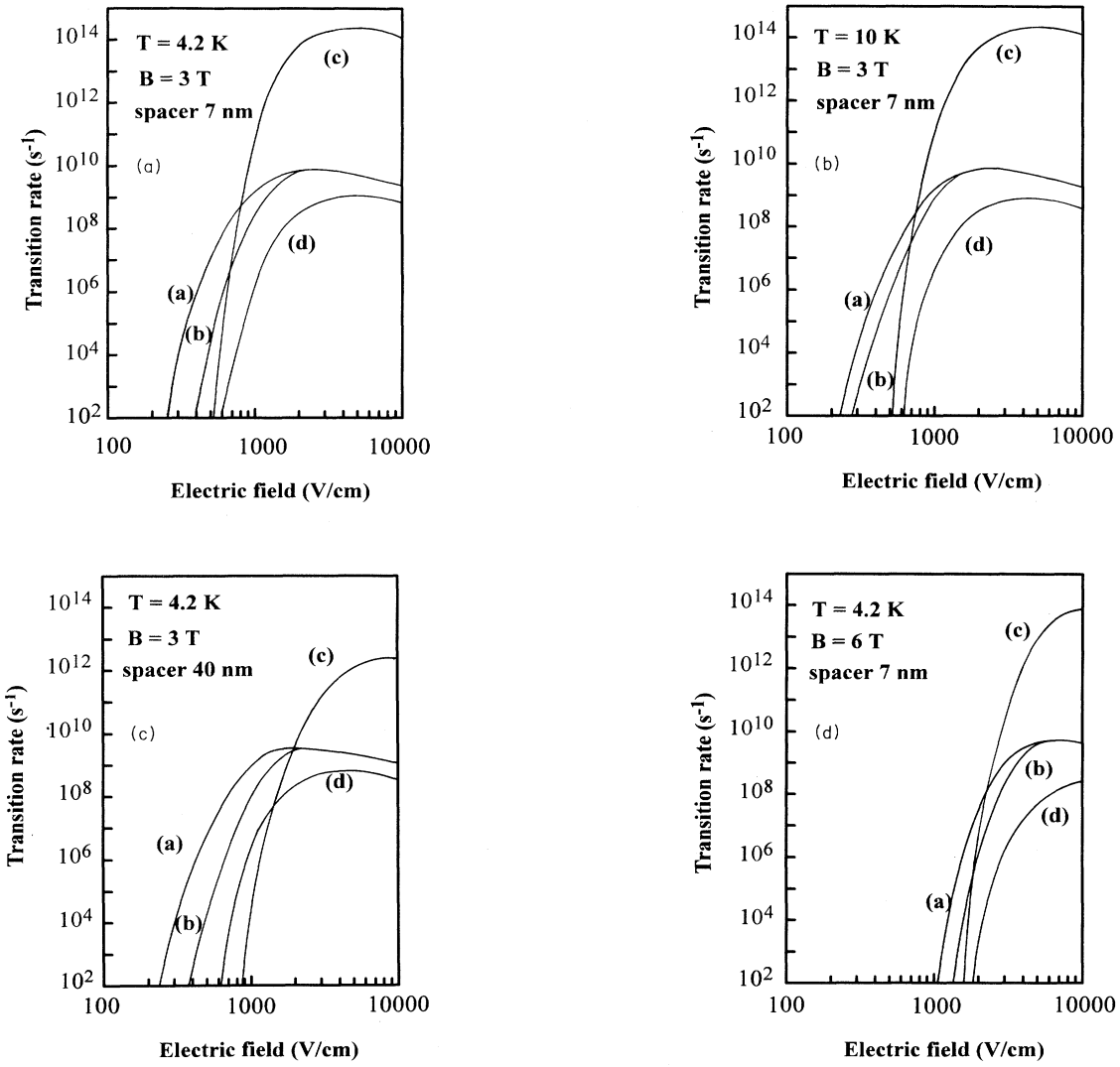

FIG. 4. Transition QUILLS rate as a function of the applied electric field, due to different scattering processes. Curve (*a*): phonon emission; curve (*b*): phonon absorption; curve (*c*): well impurities; curve (*d*): residual channel impurities. From (*a*) to (*d*), we have changed the value of the temperature, of the spacer thickness, and of the magnetic field. The parameters used in the calculations are those of sample *D*.

where ε_r is the relative dielectric constant.

One can notice that the radiative recombination process rate is directly proportional to the quantum number n. In the GaAs, for the $n=3-2$ transition, one finds for a magnetic field of 3 T, $W_0 \approx 10^5\ s^{-1}$.

6. *Numerical results of transition probabilities*

We present now the results of calculations for the transition probabilities relative to the nonradiative scattering processes described above. In Figs. 4(a), 4(b), 4(c), and 4(d), we have reported the transition probabilities of QUILLS between $n=0$ and 1 Landau levels, assisted by both phonon and impurity scattering processes, as a function of the local electric field. We have distinguished absorption and emission of phonons, as well as the two kinds of impurities (residual impurities in the well and doping impurities in the barrier). To describe the 2D electron gas of a $Ga_xAl_{1-x}As/GaAs$ heterojunction, we used in our calculations the following parameters, which correspond to sample D in the Landau emission regime: $N_s=4\times10^{11}\ cm^{-2}$, $N_{dep}=0.3\times10^{11}\ cm^{-2}$, $N_i=10^{14}\ cm^{-3}$, spacer=70 Å, $B=3$ T, $T=4.2$ K (see Table I). From Fig. 4(a) to Fig. 4(d), we have changed the value of the temperature of the spacer thickness and of the magnetic field. The first important point is that we obtain, in all cases, the same particular shape of the curves: a very steep slope in the electric-field dependence of the probabilities, with a saturation when the electric-field intensity is around 10^3 V/cm, for $B=3$ T. This steplike behavior was foreseeable: the electric field determines the slope, through X_v or k_y, of the perturbed Landau levels (Fig. 1) and as a consequence it controls the overlap of the eigenfunctions of two adjacent Landau levels. Because of the exponential decrease of these function tails, the overlap integral exponentially increases when the distance between the orbit center of two eigenfunctions becomes smaller. Hence, the probabilities exponentially increase with the slope of the Landau levels—i.e., with the electric field. In the same way, when the electric field is high enough, the overlap between two eigenstates of equal energy becomes electric-field independent: this case occurs when the distance, which separates the two orbit centers of the eigenstates, is smaller than the magnetic radius. This induces a saturation of the overlap integral and of the probabilities versus electric field (Fig. 4).

Let us now analyze in details the results, investigating separately each type of scattering processes. Concerning the interaction with acoustic phonons, it appears clear that except in the saturation domain (very high electric field), the probability of QUILLS is much larger for the emission process than for the absorption process in the whole magnetic-field range: this means that there exist statistically few phonons in this very low-temperature range. Besides, the emission of acoustic phonons is the only inelastic process able to allow the energy dissipation in the sample, until the optical-phonon emission may occur. The emission of acoustical phonon has already been studied, and it has been proved that, as a consequence of the spontaneous emission of phonons, the lattice temperature increases due to the onset of a dissipation regime.[20,23,26] A precise calculation should take into account the real lattice temperature during the heating, as previously developed by Heinonen.[20] In our case, this would require heavy calculations. However, in order to estimate the effects of an increase of the lattice temperature, we performed calculations with $T=10$ K (this could be a reasonable value for the lattice temperature under heating conditions in our experiments). We reported the results in Fig. 4(b): as expected the difference between the efficiencies of phonon emission and absorption scattering, is smaller than for 4.2 K. Consequently, we can assume that when the electric field increases, those two processes tend to be equivalent. This shows that for electron gas heating, the stronger the electric field, the larger the lattice temperature, the more efficient the phonon-scattering process.

TABLE I. Sample characteristics.

	Sample C,D: $Ga_xAl_{1-x}As$ barrier	Sample E: $Ga_xIn_{1-x}P$ barrier		
	Parameters	C	D	E
Doped	thickness (Å)	400	320	Undoped
$Ga_xAl_{1-x}As$	Al (%)	23		$Ga_xIn_{1-x}P$
Layer	N_D ($10^{18}\ cm^{-3}$)	2		Layer
Undoped	thickness (Å)	90	70	
$Ga_xAl_{1-x}As$				
spacer	Al (%)	40		
Undoped	thickness (10^3 Å)	7		10
GaAs				
channel				
$T=300$ K	N_s ($10^{11}\ cm^{-2}$)	9.2	7.0	
	μ ($10^4\ cm^2V^{-1}s^{-1}$)	0.7	0.7	
$T=77$ K	N_s ($10^{11}\ cm^{-2}$)	9.0	4.5	8.1
	μ ($10^4\ cm^2V^{-1}s^{-1}$)	12	12	3.6
$T=4.2$ K	N_s ($10^{11}\ cm^{-2}$)	6.7	3.5	3.4
	μ ($10^4\ cm^2V^{-1}s^{-1}$)	26.8	28	4.4

Concerning now the interaction with ionized impurities, Fig. 4 shows clearly that the role the residual impurities in the well is negligible. In the calculations, we used $N_i = 10^{14}$ cm^{-3}. The probability is proportional to N_i in this scattering process, and we conclude that except in the case of a rather high concentration of residual impurities ($N_i = 10^{16}$ cm^{-3}), the scattering by ionized impurities in the well has not to be taken into account.

Finally, what is remarkable in our results is the role of the ionized impurities in the barrier. In high-electric-field range, this scattering process is by far the most efficient one. Besides, as expected when the spacer thickness increases—which means the barrier impurities move away from the 2DEG—the probability of scattering decreases greatly [Fig. 4(c)]. But it is still the most efficient for a spacer thickness of 400 Å in the high-electric-field regime.

We have performed the same calculations for a higher value of the magnetic field. As expected, when the magnetic field increases, the entire curve family is shifted towards a higher electric field: the magnetic field increases the energy gap between subsequent Landau levels (Fig. 1), and consequently decreases the probability of scattering. A stronger electric field is then necessary to further incline the perturbed Landau levels so as to induce the same transition rates.

To summarize those results, we can say that the acoustic-phonon scattering is responsible for the appearance of the heating regime (lattice heating), because it appears first while increasing the electric field. Second, when the electric-field strength increases, the scattering by the ionized impurities in the barrier is the main electron heating process.

Let us now conclude with the heating process. We have shown that the electric field induces several scattering processes, and we have calculated the transition rates. Let us note that the transition rate magnitudes are physically acceptable. The scattering processes involve scattering times as small as a nanosecond to a femtosecond for the impurity scattering at high electric field. This is the order of magnitude we commonly observe in semiconductor physics. We shall now compare these values with the radiative scattering time (10^{-5} s for $B = 3$ T in GaAs). If the field-induced scattering time is smaller than the radiative one, the electrons will populate the whole Landau ladder below the optical-phonon energy, as previously discussed. In the opposite case, the radiative process is more efficient and the electrons immediately recombine as soon as they occupy an upper energy level. The heating regime cannot be achieved. Thus, one can define a typical critical field for a given type of scattering when the considered nonradiative transition rate becomes comparable to the radiative one (typically 10^5 s^{-1} in our study). The Landau emission power is expected to increase significantly when the electric field becomes stronger than the critical field.

Finally, let us make a remark on the following point: in Fig. 5, we have reported the transition probability $W_{n+1,n}$ between subsequent pairs of Landau levels (1−0, 2−1, 3−2), due to the interaction with acoustic phonons, as a function of the electric field. It appears clearly

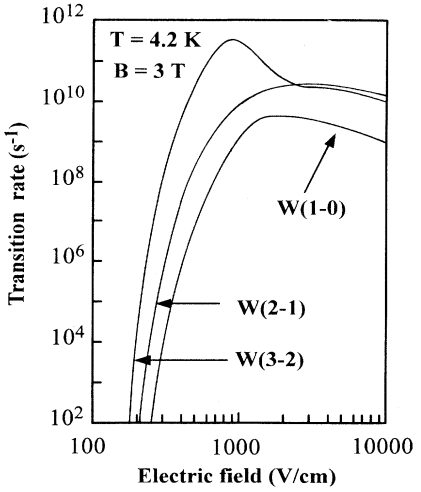

FIG. 5. Transition QUILLS rate, due to phonon scattering for different pairs of Landau levels ((1−0; 2−1; 3−2).

that for a given value of the electric field, this probability $W_{n+1,n}$ depends on the pair of involved Landau levels: the probability is much larger for the (3−2) transition than for the (1−0) one, and additional oscillations appear in the curve. This is a consequence of the overlap integral ($f_{\nu\mu}$) dependence on the Landau quantum number (one can refer to the Appendix); thus, this dependence of the transition rates with the pairs of the concerned Landau levels can exist for any type of scattering. Nevertheless, we assume that this is not of a critical importance in our study and we have considered in our following calculations that $W_{n+1,n} \approx W_{1-0}$ for all n values, which verify $(n+1/2)\hbar\omega_c < \hbar\omega_{LO}$. The reason is that we are principally interested (and especially when we compare experimental and theoretical results in Sec. III B) in the critical field that creates the appearance of the Landau emission. The critical field lies, in our case, in a steplike region of the curves (Figs. 4 and 5). Consequently, considering different $n+1-n$ transitions between Landau levels, one can expect very different transition rates at a given electric field; but, according to the very steep slope, the electric field that induces equal transition rates between different pairs $(n+1,n)$ of Landau levels can be comparable. For example, considering the case of sample D (see Sec. II C), two Landau levels are populated at the thermal equilibrium. Thus, only two transitions would be involved at the critical field: 1−0 and 2−1. Consequently, considering that $W_{n+1,n} \approx W_{1-0}$ can induce an error in the determination of the electric field smaller than 50%, this does not change our main conclusions (see Sec. III B). On the other hand, this simplifying assumption minimizes the dynamic of the heating process when the upper LL's begin to be populated: we underestimate the value of the transition rates W_{n-n+1}.

C. The statistical equilibrium and the radiative emitted power

We are now concerned with the calculation of the statistical occupation of the Landau levels, as a function of

the electric field: the competition between the scattering processes and the radiative recombination process will finally result in a steady state. To calculate the statistical distribution of the electrons, we use the following master equation:[26,28]

$$\frac{\partial \rho_\nu}{\partial t} = \sum_{\nu'} [\rho_{\nu'} W_{\nu'\nu}(1-\rho_\nu) - \rho_\nu W_{\nu\nu'}(1-\rho_{\nu'})] , \quad (29)$$

where ρ_ν is the mean value of the operator density in the state $|\nu\rangle = |n, k_y\rangle$, $W_{\nu'\nu}$ is the transition probability from state ν' to state ν induced by the phonon or by the impurity scattering.

As we are concerned by the steady-state solution (the electric field is applied during a time much larger than the characteristic time of the quantum effects), we take in the above equation $\partial\rho_\nu/\partial t = 0$. This leads to

$$\sum_{\nu'} \rho_{\nu'} W_{\nu'\nu}(1-\rho_\nu) = \sum_{\nu} \rho_\nu W_{\nu\nu'}(1-\rho_{\nu'}) , \quad (30)$$

which means that the total number of electrons getting into the state ν is equal to the total number of electrons getting out of the state ν' (Fig. 6).

We assume, therefore, that ρ_ν is independent of k_y, since we need a homogeneous solution. Then ρ_ν is equal to the Fermi-Dirac distribution function f_n of the nth LL.[26,28] If W_0 represents the transition rate due to the radiative recombination (we assume that W_0 is independent of n) and $W_{nn'}$ the transition rate due to all the scattering processes between levels n and n', the solution is, therefore, given by the final equations system:

$$f_n = \frac{f_{n+1}W_{n+1\to n} + f_{n+1}W_0 + f_{n-1}W_{n-1\to n}}{(1-f_{n-1})W_0 + (1-f_{n+1})W_{n\to n+1} + (1-f_{n-1})W_{n\to n-1} + f_{n-1}W_{n-1\to n} + f_{n+1}W_{n+1\to n} + f_{n+1}W_0} . \quad (31)$$

The solution to this problem is obtained for a given magnetic field value using a self-consistent calculation: we fix the total number of Landau levels that can be filled up under heating conditions (below the optical-phonon energy) and the total number of electrons, which determines—as we know the level degeneracy—the initial number of filled levels (without heating). We obtain the f_n values of the equilibrium, iterating the above formula.

We reported the result of the calculations in Fig. 7: we took the sample D characteristics [in order to use the theoretical results of Fig. 4(a)]; with the value of the optical-phonon energy yet introduced in Sec. II B 2 and a magnetic field $B = 2.7$ T, nine Landau levels are located below the phonon energy (from $n = 0$–8).

It appears that the filled Landau levels begin to be depopulated, whereas the empty ones begin to be populated, when the electric-field value reaches 200 V/cm. When the electric field F is larger than 600 V/cm, all the LL's initially empty contain the same density of electrons and for a value of F as high as 1000 V/cm, the 2D electrons are distributed on all the Landau levels of energy smaller than the optical-phonon energy.

The radiative emitted power P_r is known as soon as the statistical distribution of electrons is known. We write

$$P_r = \sum_n f_n(1-f_{n-1})W_0(n)\hbar\omega_c N , \quad (32)$$

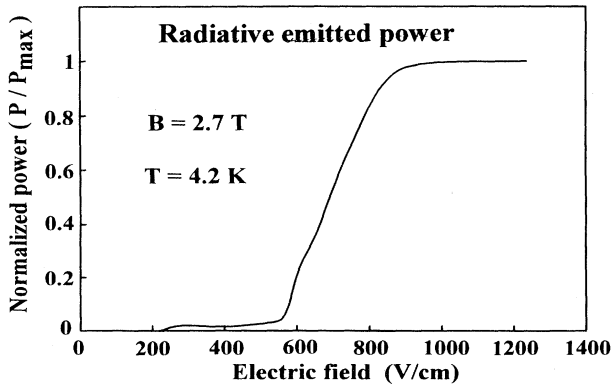

FIG. 6. Schematic balance of the radiative (W_0) and nonradiative (W) transition processes between adjacent Landau levels.

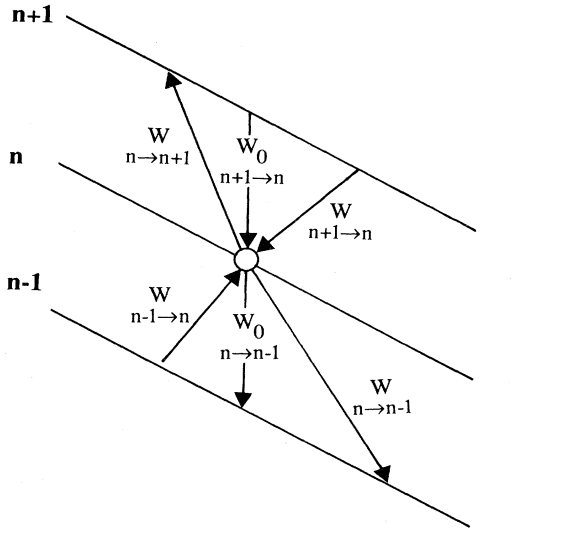

FIG. 7. Occupation probabilities of different Landau levels as a function of the electric field. The parameters used in the calculations are those of sample D. At $B = 2.7$ T and $T = 4.2$ K, two levels are filled at zero electric field, and nine levels are located below the optical-phonon energy.

where N is the total number of electrons located in the emitting zone, $W_0(n)$ the radiative recombination of the "$n-(n-1)$" transition, and $\hbar\omega_c$ the energy of the emitted photons; n indexes the Landau levels. The summation is over all the Landau levels, whose energy is smaller than the optical-phonon energy.

One problem remains: what can we take as a value for N? There are many reasons which tend to prove that the electric field F can be highly inhomogeneous in the sample (as previously discussed in the Introduction) and we should calculate P_r for each part of the sample cut in parts of equal F. Another way to solve the problem is to normalized the emitted power by its possible largest value obtained when all the considered LL's are equally populated [when the following condition is valid: $f_n=\sum_n f_n(F=0)/\sum_n 1$]. So doing,

$$P_r\max=\sum_n f_n\max(1-f_{n-1}\max)W_0(n)\hbar\omega_c N$$

and

$$\frac{P}{P_{\max}}=\frac{\sum_n f_{n+1}(1-f_n)W_0(n)}{\sum_n f_{\max}(1-f_{\max})W_0(n)} . \tag{33}$$

In order to simplify the calculations and according to the fact that we want only to evaluate correctly the REP, we take $W_0(n)\approx W_0=10^5\ \mathrm{s}^{-1}$. Then,

$$\frac{P}{P_{\max}}=\frac{\sum_n f_{n+1}(1-f_n)}{\sum_n f_{\max}(1-f_{\max})} . \tag{34}$$

This represents the physical quantity that can be easily calculated, as soon as we know the f_n values, and which we are able to measure experimentally (see Sec. III).

Let us now discuss the results of the calculations. We have reported the electric-field dependence of the total emitted power, in Fig. 8. We have performed the calculations for $B=2.7$ T and $T=4.2$ K for sample D characteristics.

For F smaller than 400 V/cm, the total radiative emitted power (REP) is negligible and due only to a very small emission between $n=1$ and 0 LLS. We saw [Fig. 4(a)], that for F larger than 500 V/cm, the transition probability due to ionized impurity scattering increases rapidly and becomes comparable to the radiative recombination probability. As a consequence, the heating of the 2D electron gas becomes efficient, the population in the higher Landau levels increases and the total REP increases sharply. This analysis shows that the ionized impurity scattering is the process responsible from a strong heating process in the 2D electron gas. We assume that the lattice temperature was 4.2 K; the scattering due to phonon absorption is a process of limited efficiency at this temperature. In a more realistic picture, the lattice temperature is certainly higher because of the emission of acoustic phonons.[20,26] Consequently, the scattering by acoustic-phonon absorption will become more efficient.

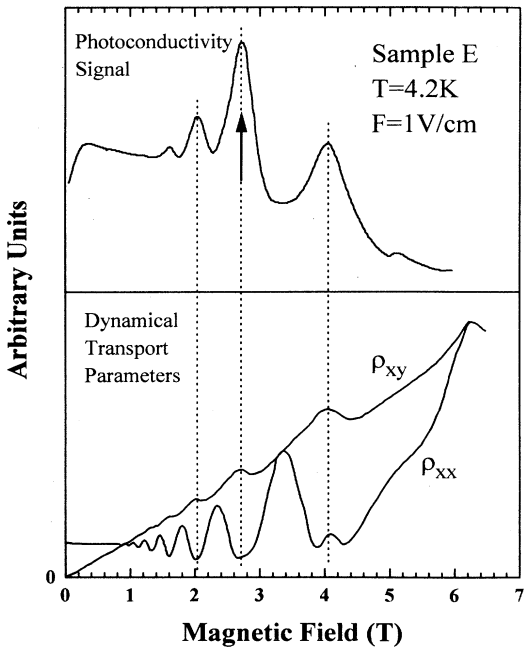

FIG. 8. Radiative emitted power as a function of the electric field. We used, in the calculations, the parameters of sample D.

One can thus expect a slope of the REP less steep than the one obtained in Fig. 8. In fact, even if the impurity scattering seems to be the most efficient one, this scattering process appears after the phonon scattering, which is the real initial cause of the breakdown of the total quantization.

We have noticed, analyzing Fig. 7, that when the heating electric field is larger than 900 V/cm, the 2D electrons are equidistributed on the Landau levels, whose energy is smaller than the optical-phonon energy. Then the QUILLS probabilities are larger than the radiative emission rate and the radiative recombination process cannot be affected by the increase of the electric field: the total REP saturates (Fig. 8). Finally, it is clear that when the electrons are equidistributed on the Landau levels, all the $(n+1-n)$ radiative recombinations are equally probable. Of course, in a more realistic picture, one has to take into account the fact that the radiative transition probability between Landau levels n and $n-1$ is proportional to n [Eq. (28)]. One can refer to the cyclotron emission study of electron masses in $Ga_xAl_{1-x}As/GaAs$ heterojunctions already published by Zawadzki *et al.*[42]

III. EXPERIMENTAL PART

A. Experimental procedure

The investigated samples were $GaAs/Ga_xAl_{1-x}As$ or $GaAs/Ga_xIn_{1-x}P$ heterojunctions grown by a metal-organic chemical-vapor-deposition (MOCVD) technique. Their characteristics are given in Table I. We performed both quantum transport and cyclotron emission experiments in magnetic field at liquid-helium temperature.

The cyclotron emission system consists of two independent 8 T superconducting coils placed in a He_4 cryostat (we took into account the stray field from one magnet in the estimation of the central field of the other). The studied sample (emitter) is placed in the center of one coil, while the detector is placed in the center of the second one. The FIR cyclotron radiation is generated by applying electric-field pulses of moderate amplitude (a few volts by cm), with varying duty cycle to avoid sample heating. The radiation was guided by a polish copper light pipe to the narrow-band detector. This detector was a magnetically tunable GaAs photoconductive detector, with a spectral resolution better than 0.5 cm^{-1}. It is sensitive, at a given magnetic field, for three well-defined energies corresponding to the $1s$-$2p^-$, $1s$-$2p^0$, and $1s$-$2p^+$ transitions of a residual single shallow donor in bulk GaAs. In zero magnetic field, there is only one $1s$-$2p$ energy equal to 4.43 meV (35.7 cm^{-1}). In these experiments, the emitter magnetic field is tuned and the detector is kept at a constant field. In this operating mode, the detector signal (detector photocurrent) reaches a maximum when the cyclotron energy coincides with one of the three transition energies $1s$-$2p^{-/0/+}$.

The FIR spectra presented in this paper have been obtained in the following way: we have divided the detector photocurrent by the emitted current; this is equivalent to that normalized by the applied electric power. Transport experiments were performed by the ac method,[41,42] in order to measure the resistivity components ρ_{xx} and ρ_{xy} in the same electrical conditions as those use for the heating of the 2D electrons in the cyclotron emission experiments.

B. Experimental results and discussion

Figure 9 represents the FIR spectrum normalized by the electric power input obtained for sample E, with a mean heating electric field F of 1 V/cm, and detected at 4.43 meV. For this low-electric-field value, we observe several lines (maxima) in the spectrum. In Fig. 9, we have reported also the transport parameters ρ_{xx} and ρ_{xy} measured by the ac method with the same electric field $F=1$ V/cm. It appears clearly that under those heating conditions, the QHE is observable and the maxima of FIR emissions coincide with the minima of ρ_{xx}, i.e, with the plateaus of ρ_{xy}. This shows that the observed emitted power amplification is due to the modification of the current path geometry that induces an enhancement of the local electric field in the QHE plateaus regime.[9-16,52] Indeed, the multiple FIR emission automatically disappears when the heating electric field is high enough to destroy the total quantization and consequently to destroy the QHE: the current path geometry is then magnetic-field independent (Fig. 10). This first remarkable result shows that the important physical parameter is the local electric field, and that the mean electric field applied to the sample has no physical meaning.

To evaluate the discrepancy that exists between the mean and the local electric field, we have performed the following experiments: we measured the emission power at the resonance ($B \approx 2.7$ T) as a function of the mean

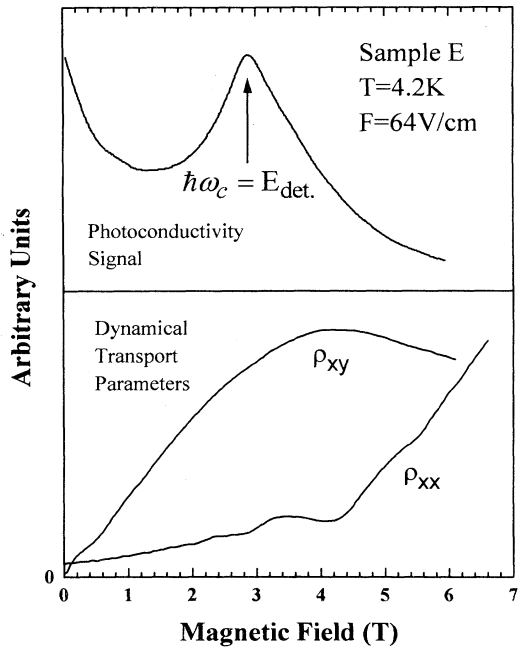

FIG. 9. Cyclotron emission signal and quantum transport parameters in $Ga_xAl_{1-x}As/GaAs$ heterojunctions (sample E) obtained in the same condition of heating: the mean electric field applied is equal to 1 V/cm. The arrow indicates the cyclotron emission peak.

electric field, applied on two different points of contacts of sample C (see Figs. 11, 12, and 14): the ratio of the distances $d(12)/d(56)$, equals 11.6. The dependence of P/P_{max} as a function of the mean electric field is similar, in both experimental cases, to the one obtained by the theoretical investigations (Fig. 8). However, the absolute value of the electric field, which gives the saturation, de-

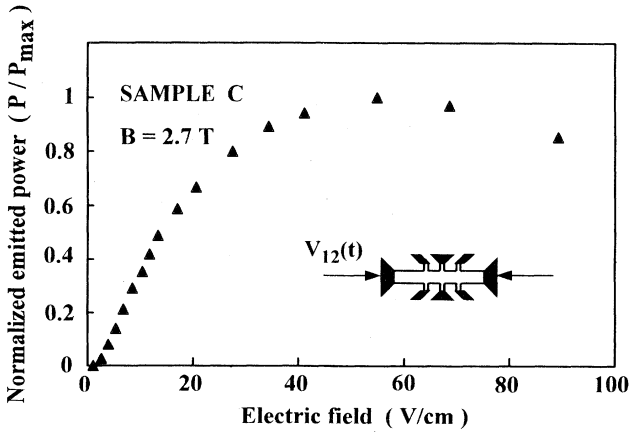

FIG. 10. Cyclotron emission signal and quantum transport parameters in $Ga_xAl_{1-x}As/GaAs$ heterojunctions (sample E), obtained in the same condition of heating: the mean electric field applied is equal to 64 V/cm. The arrow indicates the cyclotron emission peak.

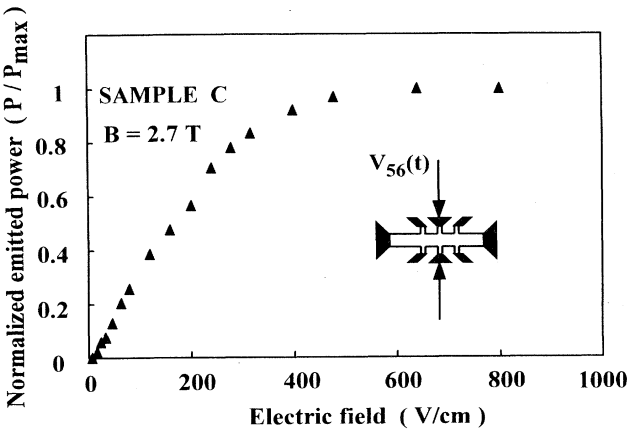

FIG. 11. Experimental values of the normalized radiative emitted power, as a function of the electric field under longitudinal configuration.

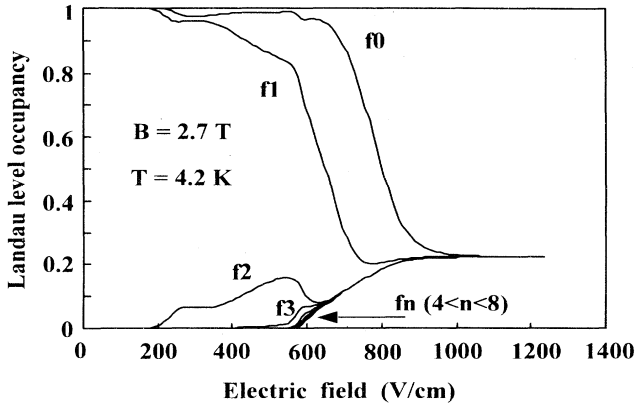

FIG. 13. Theoretical and experimental values of the normalized emitted power, as a function of the electric field. The discrepancy is attributed to the nonhomogeneity of the potential distribution in the structure.

pends on the heating configuration. For the geometry "*a*" (electric field applied along the axis of the sample), the saturation is obtained for 40 V/cm, when, for geometry "*b*" (electric field normal to the axis of the sample), the saturation is obtained for 400 V/cm. This discrepancy corroborates the fact that the measured mean electric field is not a good physical parameter for describing the heating of 2D electrons in the cyclotron emission of 2DEG: the value of F, which gives the saturation, should be the same in both cases.

In order to compare theoretical and experimental values of the electric field that induces the emission, we performed similar investigations on sample D with a shunted bridge geometry as previously used by Robert *et al.*[43] to study the zero resistance state in GaAs-$Ga_xAl_{1-x}As$ heterojunctions (Fig. 13). In this quasi-Corbino geometry, the electric field is theoretically more homogeneous than in the classical Hall bar geometry. As shown on Fig. 13, we have applied the electric field perpendicularly to the loop of the Corbino geometry. We have reported on this figure, the experimental and theoretical dependence of the normalized emitted power as a function of the mean electric field. We performed the calculations yet described in Sec. II C and we took the sample D characteristics. The cyclotron emission experiments have been performed with a magnetic field of 1 T on the detector, and we used the $1s$-$2p^+$ line (5.84 meV); 3.7 T was applied to the emitter (sample D). We still observe a huge discrepancy that corroborates our previous experimental results: theoretical and experimental results can be consistent only if we state that the local electric field can be as high as 1 kV/cm in some parts of the sam-

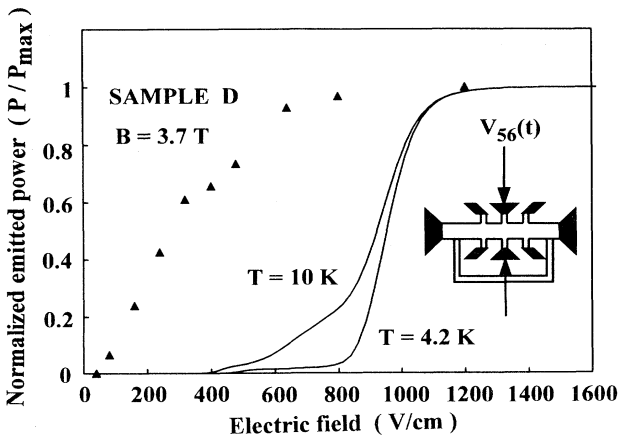

FIG. 12. Experimental values of the normalized radiative emitted power, as a function of the electric field under transverse configuration.

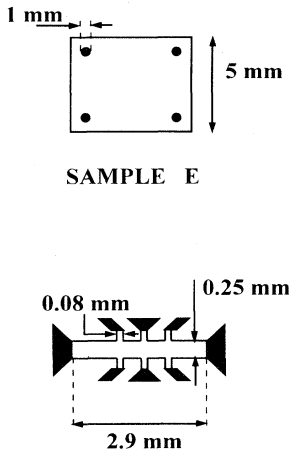

FIG. 14. Geometric sample characteristics.

TABLE II. Cyclotron emission characteristics.

	Sample	Contact length (mm)	Estimated emitting surface (μm^2)	Sample surface (μm^2)
C	longitudinal polarization	0.25	150	750×10^3
	transverse polarization	0.08	30	750×10^3
E		6	2000	25×10^6

ple to induce the emission, and, consequently, that the mean electric field does not have any physical meaning, because of the potential inhomogeneity. This implies that in the rest of the sample, the electric field would be much smaller and consequently too small to induce QUILLS processes. This means that the real surface of the FIR emission would be much smaller than the sample surface. We have done experiments that tend to corroborate this assumption: in order to estimate the surface of the FIR emission, we have measured the emitted power in the saturation regime, and compared it to the theoretical value assuming that, in this regime, all the 2D electrons participate in the cyclotron emission. As we know the detector sensitivity ($\approx 0,1$ A/W), we could measured easily the emitted power P_e. Then, assuming that the total number N of electrons, which effectively participate in the emission process, is equal to $(N_s \times S)$ (S is the surface of emission), one can easily deduce the value of S by writing

$$P_{\text{exp}} = \sum_n f_{n+1}(1-f_n)W_0(n)\hbar\omega_c N_s S \ ,$$

where the summations over n concern all the Landau levels whose energy is smaller than the optical-phonon energy, and P_{exp} is the experimental value of the emitted power.

We have summarized the results in Table II: it appears clear that in each case, the surface of emission is approximately 10^4 times smaller than the surface of the sample, which corroborates our model. We can now state that this "hot spot" behavior is similar to the one brought to light by Russel *et al.*[44] and Klaβ *et al.*,[45] or more recently by Shashkin *et al.*[53] More, in the present study, we measure and calculate the emitted power in the far-infrared frequency range, and we deduce from the optical measurement surface of such a spot. Besides we prove that potential inhomogeneities (i.e., intense electric field) can induce such a FIR radiation, due to QUILLS processes. One important area that we must question remains. This "hot spot" behavior that we observe is not directly correlated to the plateaus regime of the QHE, as previously assumed by Klaβ *et al.*: in our experiments of cyclotron emission, the breakdown of the QHE has already occurred . Nevertheless, we think that the behavior that we put into light can be highly enhanced in the plateaus regime, due to the very particular shape of the current path geometry. Nevertheless, we think that the original cause of the creation of such a zone might reside in the general problem of the injection of electrons in a 2D gas, independent of the Hall conditions. This will emphasize the role of contacts in the QHE, as yet demonstrated by a great amount of works in the recent years.[46–50] One can actually remark that the surface of emission that we found, is roughly proportional to the size of the sample constant (see Table II and Fig. 14).

We would like, finally, to bring to light that this theoretical study of the QUILLS processes allows us to define a critical electric field for the Landau emission phenomenon. This phenomenon is strongly correlated to the breakdown of the QHE (breakdown of the total quantization), a breakdown for which one can adopt the Landau emission critical field. Then the QUILLS processes could allow the calculation of the critical field and consequently, as concluded by Balaban *et al.*,[52] of the breakdown current in the QHE regime.

IV. CONCLUSION

The theoretical and experimental studies that we made, of the heating of 2D electrons, by an in-plane electric field, give us rich and useful information for the understanding of the Landau emission in 2D electron gas, as well as for the knowledge of the breakdown of the quantum Hall effect.

(i) The analysis of the dependence of the transition probabilities with electric-field intensity shows that the real heating of the 2D electrons is due to the scattering by ionized impurities intentionally introduced in the barrier; the apparent heating (lattice heating) is due to the emission of acoustic phonons.

(ii) Landau emission and quantum transport experiments, coupled with the calculations of the radiative emission power, clearly establish that the electric field in a 2D electron gas submitted to a quantizing magnetic field is highly inhomogeneous: very high value can be reached for the local electric field, even out of the plateaus regime of the quantum Hall effect. This local electric field is responsible for the existence of the inter-Landau-level scattering (the consequences are both the Landau emission process and the breakdown of the quantum Hall effect).

ACKNOWLEDGMENTS

We thank Dr. J. P. André from Laboratoire d'Electronique et de Physique Appliquée, Philips, for providing the samples, and Professor M. Dyakonov from the Ioffe Institut in St. Petersburg and Professor W.

Zawadzki from the Polish Institute of Physics in Warsaw for helpful discussions.

APPENDIX: CALCULATIONS OF THE OVERLAP INTEGRALS $|f_{\nu\mu}(q)|^2$

The integral $\langle \nu|e^{i\mathbf{q}\cdot\mathbf{r}}|\mu\rangle$ can be decomposed in a three independent terms product:

$$\langle \nu|e^{i\mathbf{q}\cdot\mathbf{r}}|\mu\rangle = \left\{\int_z \chi_0^2(z)e^{iq_z z}dz\right\} \times \left\{\int_y \frac{e^{-ik'_y y}}{\sqrt{L_y}} e^{iq_y y}\frac{e^{ik_y y}}{\sqrt{L_y}}dy\right\} \times \left\{\int_x \Phi_{n'}(x-X_\nu)e^{iq_x x}\Phi_n(x-X_\nu)dx\right\} .$$

The first term was calculated by Lassnig and Zawadzki,[51] taking the Fang and Howard functions:

$$\left|\int_z \chi_0^2(z)e^{iq_z z}dz\right|^2 = \frac{1}{\left[1+\frac{q_z^2}{b^2}\right]^3} ,$$

where

$$b=\left[\frac{12m^* e^2}{\varepsilon_r\varepsilon_0\hbar^2}\left(N_{\text{dep}}+\tfrac{11}{32}N_s\right)\right]^{1/3} \approx 3.10^8 \text{ m}^{-1} .$$

The second term is 1 when $q_y = k'_y - k_y$, and 0 otherwise. The third term is analytically expressed for given n and n'. We first change the variable system: $x = x - X_\nu$, and we call $X_0 = X_{\nu'} - X_\nu$. We have to calculate

$$I_{n,n'} = \int_x \Phi_n(x-X_0)e^{iq_x x}\Phi_{n'}(x)dx .$$

The first four Landau eigenfunctions Φ_n are

$$\Phi_0(x)=\left[\frac{\beta}{\pi}\right]^{1/4} e^{-\beta x^2/2} \quad \text{with } \beta=\frac{m^*\omega}{\hbar}=\frac{eB}{\hbar} ,$$

$$\Phi_1(x)=\left[\frac{4\beta^3}{\pi}\right]^{1/4} x e^{-\beta x^2/2} ,$$

$$\Phi_2(x)=\left[\frac{\beta}{4\pi}\right]^{1/4} (2\beta x^2-1)e^{-\beta x^2/2} ,$$

$$\Phi_3(x)=\left[\frac{\beta^3}{9\pi}\right]^{1/4} x(2\beta x^2-3)e^{-\beta x^2/2} ,$$

and the integrals $I_{n,n'}$ can be expressed as functions of the integrals $J_n = \int_{-\infty}^{+\infty} x^n e^{-\beta x^2} e^{iQx}dx$. These are easily obtained by integrating in the complex plane. For example, the two first terms are

$$J_0=\left[\frac{\pi}{\beta}\right]^{1/2} e^{-Q^2/4\beta} ,$$

$$J_1=\frac{iQ}{2\beta}\left[\frac{\pi}{\beta}\right]^{1/2} e^{-Q^2/4\beta} .$$

The following terms of the suite are more and more complicated, but can be known without difficulties. Then, the calculations of the $I_{n,n'}$ is fastidious but as well rather simple. Taking the modulus, one then obtains $|f_{\nu\mu}(q)|^2$.

We call

$$\alpha^2=\frac{q_y^2}{\beta} \text{ and } \bar{q}^2=\frac{q_x^2}{\beta} .$$

Then, the first integrals are

$$|\langle\Phi_0|e^{iq_x x}|\Phi_1\rangle|^2=\tfrac{1}{2}(\alpha^2+\bar{q}^2)e^{-(\alpha^2+\bar{q}^2)/2} ,$$

$$|\langle\Phi_1|e^{iq_x x}|\Phi_2\rangle|^2=\tfrac{1}{16}\{16\bar{q}^2-8\bar{q}^4+\bar{q}^6 +\alpha^2(16-16\bar{q}^2+3\bar{q}^4) +\alpha^4(-8+3\bar{q}^2)+\alpha^6\} \times e^{-(\alpha^2+\bar{q}^2)/2} ,$$

$$|\langle\Phi_2|e^{iq_x x}|\Phi_3\rangle|^2=\tfrac{1}{24}\{A_0+\alpha^2A_2+\alpha^4A_4+\alpha^6A_6+\alpha^8A_8 +\alpha^{10}A_{10}+\alpha^9A_9+\alpha^7A_7+\alpha^5A_5 +\alpha^3A_3+\alpha A_1\}e^{-(\alpha^2+\bar{q}^2)/2} ,$$

where

$$A_0=\frac{\bar{q}^{10}}{16}+36\bar{q}^2+9\bar{q}^6-36\bar{q}^4 , \quad A_9=-\tfrac{3}{2} ,$$

$$A_2=\frac{\bar{q}^8}{16}-\bar{q}^7-8\bar{q}^6+45\bar{q}^4-72\bar{q}^2+36 , \quad A_7=-6-5\bar{q}^2 ,$$

$$A_4=\tfrac{9}{4}\bar{q}^6-\bar{q}^5-\tfrac{21}{2}\bar{q}^4+36\bar{q}^2-36 ,$$

$$A_5=12-6\bar{q}^2-\tfrac{13}{2}\bar{q}^4+\bar{q}^5 ,$$

$$A_6=4\bar{q}^4+3\bar{q}^2 , \quad A_3=6\bar{q}^4-3\bar{q}^6+\bar{q}^7 ,$$

$$A_8=\tfrac{37}{16}\bar{q}^2+\tfrac{11}{2} , \quad A_1=-12\bar{q}^4+6\bar{q}^6 ,$$

$$A_8=\tfrac{37}{16}\bar{q}^2+\tfrac{11}{2} .$$

Finally, one can write

$$|f_{\nu\mu}(q)|^2=\frac{1}{\left[1+\frac{q_z^2}{b^2}\right]^3}\times|\langle\Phi_n|e^{iq_x x}|\Phi_{n'}\rangle|^2 ,$$

where $|\langle\Phi_n|e^{iq_x x}|\Phi_{n'}\rangle|^2$ is given by the above expressions.

[1]E. Gornik, Phys. Rev. Lett. **29**, 595 (1972).
[2]E. Gornik, in *Narrow-Gap Semiconductor Physics and Applications,* edited by J. Ehlers, Lecture Notes in Physics Vol. 133 (Springer-Verlag, Berlin, 1979), p. 160.
[3]E. Gornik, Physica **127B**, 95 (1984).
[4]E. Gornik, in *Application of High Magnetic Fields in Semiconductor Physics,* edited by G. Landwehr (Springer-Verlag, Berlin, 1982), p. 248.
[5]K. L. Kobayashi, K. F. Komatsubara, and E. Otsuka, Phys. Rev. Lett. **30**, 702 (1973).
[6]E. Gornik, W. Seidenbush, R. Christanell, R. Lassnig, and C. R. Pidgeon, Surf. Sci. **196**, 339 (1982).
[7]J. L. Robert, A. Raymond, J. Y. Mulot, C. Bousquet, J. P. André, W. Knap, M. Kubisa, W. Zawadzki, E. Gornick, and W. Seidenbush, in *Proceeding of the 19th International Conference on the Physics of Semiconductors,* edited by W. Zawadzki (Institute of Physics, Polish Academy of Sciences, Warsaw, 1988), Vol. 1, p. 197.
[8]W. Knap, S. Huant, C. Chaubet, and B. Etienne, Superlatt. Microstruct. **8**, 3 (1990).
[9]H. Z. Zheng, D. C. Tsui, and A. M. Chang, Phys. Rev. B **32**, 5506 (1985).
[10]G. Ebert, K. von Klitzing, and G. Weimann, J. Phys. C **18**, 257 (1985).
[11]P. F. Fontein, Ph.D. thesis, Eindhoven University, 1990; Surf. Sci. **229**, 47 (1990).
[12]H. Wolf, G. Hein, L. Bliek, G. Weimann, and W. Schlapp, Semicond. Sci. Technol. **10**, 1046 (1990).
[13]O. Heinonen and P. L. Taylor, Phys. Rev. B **32**, 633 (1985).
[14]A. H. Mac Donald and P. Sreda, Phys. Rev. B **29**, 1616 (1984).
[15]A. H. Mac Donald, T. M. Rice, and W. F. Brinkman, Phys. Rev. B **28**, 3648 (1983).
[16]M. I. Dyakonov and F. G. Pikus, Solid State Commun. **83**, 413 (1991).
[17]H. Sakaki, K. Hirakawa, J. Yoshino, S. P. Svensson, Y. Sekiguchi, T. Hotta, and S. Nishii, Surf. Sci. **142**, 306 (1984).
[18]M. E. Cage, R. F. Dziuba, B. F. Field, E. R. Williams, S. M. Girvin, A. C. Gossard, D. C. Tsui, and R. J. Wagner, Phys. Rev. Lett. **51**, 1374 (1983).
[19]L. Bliek *et al.*, Semicond. Sci. Technol. **1**, 110 (1986).
[20]O. Heinonen, P. L. Taylor, and S. M. Girvin, Phys. Rev. B **30**, 3016 (1984).
[21]P. S. S. Guimaraes, L. Eaves, F. W. Sheard, J. C. Portal, and G. Hill, Physica **134B**, 47 (1985).
[22]L. Eaves and F. W. Sheard, Semicond. Sci. Technol. **1**, 346 (1986).
[23]L. Bliek, Semicond. Sci. Technol. **6**, 188 (1991).
[24]G. Ebert, K. von Klitzing, K. Ploog, and G. Weimann, J. Phys. C **16**, 5441 (1983).
[25]M. I. Dyakonov, Solid State Commun. **78**, 817 (1991).
[26]D. Calecki, C. Lewiner, and P. Nozières, J. Phys. (Paris) **38**, 169 (1977).
[27]M. Büttiker, Phys. Rev. B **38**, 9375 (1988).
[28]M. Helm and E. Gornik, Phys. Rev. B **39**, 6212 (1989).
[29]G. Mahan, in *Polarons in Ionic Crystals and Polar Semiconductors,* edited by J. T. Devreese (North-Holland, Amsterdam, 1972).
[30]J. Bardeen and W. Shockley, Phys. Rev. **80**, 72 (1950).
[31]J. J. Harris *et al.*, Surf. Sci. **229**, 113 (1990).
[32]L. M. Roth and P. N. Argyres, in *Physics of III-V Compounds,* edited by R. K. Willardson and A.C. Beer, Semiconductors and Semimetals Vol. 1 (Academic, New York, 1966), Chap. 6.
[33]T. Kawamira and Das Sarma, Phys. Rev. B **42**, 3725 (1990).
[34]A. Mooradian and G. B. Wright, Solid State Commun. **4**, 431 (1966).
[35]T. Ando, A. B. Fowler, and F. Stern, Rev. Mod. Phys. **54**, 437 (1982).
[36]G. Bastard, *Wave Mechanics Applied to Semiconductor Heterostructures* (Les Editions de Physique, Les Ulis, 1992).
[37]M. Helm, E. Gornik, A. Black, G. R. Allan, C. R. Pidgeon, K. Mitchell, and G. Weimann, Physica **134B**, 323 (1985).
[38]K. Muro, S. Narita, S. Hiyamizu, K. Nambu, and H. Hashimoto, Surf. Sci. **113**, 321 (1982).
[39]W. Zawadzki, in *Narrow Gap Semiconductors Physics and Applications,* edited by J. Ehlers, Lecture Notes in Physics Vol. 133 (Springer-Verlag, Berlin, 1979), p. 85.
[40]See, for example, *Quantum Field Theory,* edited by F. Mandi and G. Shaw (Wiley, New York, 1984).
[41]A. Raymond and C. Chaubet, SPIE Proc. **1362**, 275 (1990).
[42]W. Zawadzki, C. Chaubet, D. Dur, W. Knap, and A. Raymond, Semicond. Sci. Technol. **9**, 320 (1994).
[43]J. L. Robert, A. Raymond, J. Y. Mulot, C. Bousquet, W. Zawadzki, M. Kubisa, and J. P. André, Phys. Rev. B **39**, 1832 (1989).
[44]P. A. Russel, F. F. Ovali, N. P. Hewett, and L. J. Challis, Surf. Sci. **229**, 54 (1990).
[45]U. Klaβ, W. Dietsche, K. von Klitzing, and K. Ploog, Z. Phys. B **82**, 351 (1991).
[46]G. Müller *et al.*, Phys. Rev. B **42**, 7633 (1990).
[47]S. Komiyama and H. Hirai, Phys. Rev. B **40**, 7767 (1989).
[48]R. J. Haug, K. von Klitzing, K. Ploog, and P. Streda, Surf. Sci. **229**, 229 (1990).
[49]S. Komiyama *et al.*, Phys. Rev. B **45**, 11 085 (1992).
[50]R. J. Haug, Semicond. Sci. Technol. **8**, 131 (1993).
[51]R. Lassnig and W. Zawadzki, Phys. Rev. B **31**, 8076 (1985).
[52]N. Q. Balaban, U. Meirav, H. Shtrikman, and Y. Levinson, Phys. Rev. Lett. **71**, 1443 (1993).
[53]A. A. Shashkin, A. J. Kent, P. A. Harrison, L. Eaves, and M. Henini, Phys. Rev. B **49**, 5379 (1994).